analytical chemistry

Article

pubs.acs.org/ac

Noninvasive Analysis of Thin Turbid Layers Using Microscale Spatially Offset Raman Spectroscopy

Claudia Conti,*[,†] Marco Realini,[†] Chiara Colombo,[†] Kay Sowoidnich,[‡] Nils Kristian Afseth,[§] Moira Bertasa,[†] Alessandra Botteon,[†] and Pavel Matousek*[,‡]

[†]Institute for the Conservation and Valorization of Cultural Heritage (ICVBC), National Research Council, Via Cozzi 53, 20125, Milano, Italy

[‡]Central Laser Facility, Research Complex at Harwell, STFC Rutherford Appleton Laboratory, Harwell Oxford, OX11 0QX, United Kingdom

[§]Nofima-Norwegian Institute of Food, Fisheries and Aquaculture Research, PB 210, N-1431 Ås, Norway

ABSTRACT: Here, we demonstrate, for the first time, the extension of applicability of recently developed microscale spatially offset Raman spectroscopy (SORS), micro-SORS, from the area of cultural heritage to a wider range of analytical problems involving thin, tens of micrometers thick diffusely scattering turbid layers. The method can be applied in situations where a high turbidity of layers prevents the deployment of conventional confocal Raman microscopy with its depth resolving capability. The method was applied successfully to detect noninvasively the presence of thin, highly turbid layers within polymers, wheat seeds, and paper. An invasive, cross sectional analysis confirmed the micro-SORS findings. Micro-SORS represents a new Raman imaging modality expanding the portfolio of noninvasive, chemically specific analytical tools.

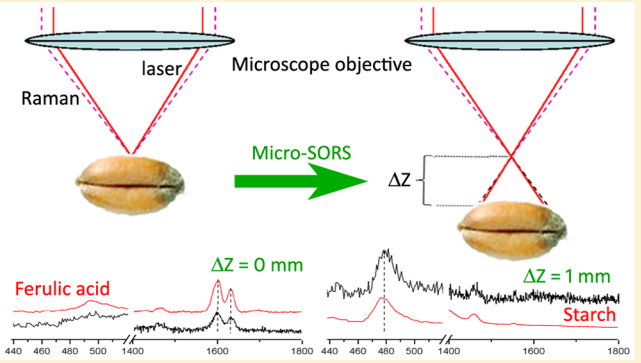

Chemically specific analysis of diffusely scattering, microscale stratified layers by nondestructive and noninvasive means is an important analytical area with wide outreach and impact. In this field, confocal Raman microscopy is a powerful analytical technique with wide use spanning from biomedical and biological diagnosis and analysis to material sciences, forensic sciences, semiconductor, pharmaceutical, and geology research and manufacture to name a few.[1] Although applicable to deep noninvasive probing with transparent or semitransparent materials, its applicability to scanning within turbid (diffusely scattering) samples is severely limited due to its inability to form direct optical images of inner components of such samples. With highly turbid matrices, which are often encountered with paints, coatings, or biological interfaces, the depth penetration can be restricted to distances as short as several micrometers. Many analytical problems can thus be outside the reach of conventional Raman microscopy. Very recently, we have developed a new concept in Raman microscopy, micro-spatially offset Raman spectroscopy (SORS),[2,3] for probing of highly turbid samples enabling one to breach the limit of the accessible depths of conventional confocal Raman microscopy. The method builds on earlier advances in a related technique developed in recent years, SORS,[4−6] by merging SORS with microscopy concepts. Generally, (micro-)SORS and related approaches utilize the properties of the diffusely scattered component of light in analogy with similar concepts used in NIR absorption[7−10] and fluorescence tomography.[11,12] However, Raman spectroscopy offers much richer chemical information, a property which unlocks a multitude of new applications.

Unlike the standard SORS, micro-SORS permits one to resolve very thin layers, on a micrometer scale as opposed to millimeter scale. It has been shown theoretically that in turbid (diffusely scattering) media its penetration depth can be up to 2 orders of magnitude larger than the accessible depths of conventional confocal Raman microscopy.[13] A similar observation was also made with conventional SORS on a macroscale in relation to conventional Raman spectroscopy.[6] Initially, the micro-SORS concept was specifically developed for probing painted layers in art.[2,3] In this study, we demonstrate, for the first time, that the applicability of this new method stretches far beyond the cultural heritage and probing of painted layers. We highlight its potential in several important areas including biology, material sciences (i.e., polymer and paper research), and quality control. These uses are exemplified here conceptually by applying the technique to the noninvasive analysis of a stratified polymer system, a glossy paper and a wheat seed.

Polymer layers and films are an important class of materials omnipresent in our daily lives. Multiple layers are often used in manufacture to facilitate various functions and properties of the final product; for example, in food packaging, the container must

Received: March 20, 2015
Accepted: May 11, 2015
Published: May 22, 2015

DOI: 10.1021/acs.analchem.5b01080
Anal. Chem. 2015, 87, 5810−5815

not interact chemically with the content: it must provide an effective chemical barrier from the external environment, and it also needs to provide desired mechanical properties and durability. Such multifunctionality is often achieved by multilayering of different polymers on top of each other. These layers can be highly diffusely scattering and as such not accessible by conventional Raman microscopy. The analysis of these layers is important in many areas including polymer research and manufacture quality control.

The structural analysis of paper and pulp chemistry, in general, is another important analytical area where both infrared and Raman spectroscopy are essential analytical tools.[14] These can include the studies of cellulose, hemicellulose, lignin, thermal- and photoinduced oxidation, cross-linking, and various chemical treatments of pulp and paper products. However, high turbidity of samples can preclude deep internal analysis by noninvasive means. Here, we demonstrate that micro-SORS can facilitate this capability in this area too.

Grain composition is an important quality marker in food processing. Not only protein and carbohydrate contents, but also starch composition and other minor components could affect the quality of the grains, and linking seed composition as well as seed development during processing and storage with end quality is of major importance. In addition, identification of diseases at an early stage is of significant importance for the grain producers, which calls for rapid and nondestructive methods for characterization of inner grain components. Raman and IR spectroscopies have been extensively studied for unravelling the microstructure of grains and their components. As early as 1993, Wetzel and Reffner published a study that summarizes the early work of using spatially resolved FT-IR microspectroscopy to examine the microstructure of wheat kernels.[15] Recently, Jaaskelainen et al.[16] used Raman microscopy to study the endosperm and aleurone cell structure in barley and wheat grains. A common drawback when performing IR and Raman microspectroscopy is the need for sample sectioning prior to microspectroscopic analysis. This is a destructive and time-consuming process, and for grains, the occurrence of cracks and other artifacts due to sectioning is frequently taking place. A nondestructive technique, in order to rapidly characterize chemical components within a grain quantitatively or to monitor anomalies, would thus be of a significant advantage. Near-infrared spectroscopy is frequently used in the grain industry to quantify major grain components like starch, lipids, and moisture. However, even though the technique can be used to penetrate through single intact grains, the level of information to extract from NIR spectra is limited. Transmission Raman spectroscopy is a relevant alternative that could possibly provide information from inside grains, but no spatial information could be obtained from this technique. With micro-SORS, however, one could expect to mimic the information obtained from microspectroscopy of sectioned kernels, providing spatial information from within the kernel.

EXPERIMENTAL SECTION

Micro-SORS Technique. In its simplest form, the micro-SORS concept, defocusing micro-SORS derived from early research into defocusing SORS,[17−19] is based on acquiring several Raman spectra using a standard confocal Raman microscope; one spectrum with a sample in a conventional "imaged" position and the other spectra in "defocused" positions, in which both the laser illumination and Raman collection areas on the sample surface are enlarged (Figure 1). The latter is facilitated by moving the sample away from the microscope objective by "defocusing distance Δz". (The same effect could also be achieved by moving the sample toward the microscope objective although it is advisable to move the sample away from the objective not to have the Δz range restriction and to avoid the risk of inadvertently impacting the microscope objective with the sample.) The "imaged" spectrum is dominated by the surface layer contributions whereas the "defocused" spectra have a higher contribution, in relative terms, from sublayers compared with the "imaged" spectrum. This is in analogy with the standard SORS method where the former represents a zero spatial offset spectrum and the latter a nonzero spatial offset spectrum.[4]

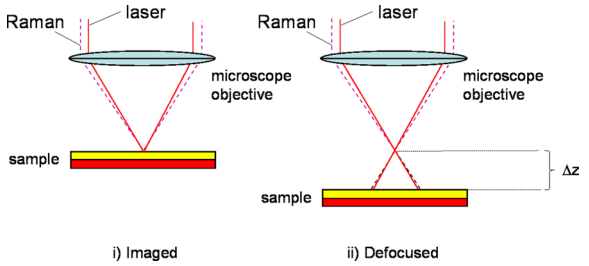

Figure 1. Schematic diagram of micro-SORS measurement consisting of (i) imaged and (ii) "defocused" acquisitions.

A pure Raman spectrum of the sublayer can be retrieved numerically simply by scaled subtraction of the "imaged" spectrum from the "defocused" spectrum canceling the contribution of the surface layer. A pure Raman spectrum of the surface layer is in turn obtained by a scaled subtraction of the "defocused" spectrum from the "imaged" spectrum canceling subsurface features. Multiple layers can also be analyzed by this method. For a system containing $n > 2$ layers, a number of at least n spectra recorded at different Δz positions are required.[2]

To compensate for the loss of signal in the "defocused" position, higher laser powers can be used. This is permitted because of the enlarged laser spot size present in this position. In addition, acquisition times can also be increased if desirable.

Specimens. The first specimen (S1) is an artificially assembled two-layer polymeric system. Both layers were highly turbid and opaque in appearance. The top layer was a polytetrafluoroethylene (PTFE) tape (75 μm thick) placed over a 150 μm thick sublayer of a plastic drinking cup made of polypropylene (PP). The second specimen (S2) is a single-side coated paper sheet consisting of multiple micrometric layers; micro-SORS analysis was applied both at the front (coated) and at the back side (nonglossy). The third example (S3) is a wheat seed of the variety "Olivin", a winter wheat variety grown in Norway, representing use in biology. Cross sections have been prepared for S2 and S3 to deduce the internal structure and chemical composition directly and provide comparative data for micro-SORS.

Micro-SORS Measurements. Micro-SORS analyses were carried out using a Renishaw In-Via Raman microscope with 1200 grooves/mm grating, Peltier cooled CCD, 50× objective with numerical aperture 0.45 (Nikon, L Plan, SLWD, 50×/0.45, ∞/0 WD 17), and two selected excitation wavelengths, 830 and 514 nm. The 830 nm measurements used a laser power at the sample of up to 36 mW and the 514 nm measurements a power of up to 7.6 mW. The micro-SORS measurements of plastic layers were carried out at 514 nm. Due to fluorescence interference at this wavelength, the paper and wheat seed studies were conducted at 830 nm. No confocal pinhole was employed in the micro-SORS system in any of the measurements presented

DOI: 10.1021/acs.analchem.5b01080
Anal. Chem. 2015, 87, 5810−5815

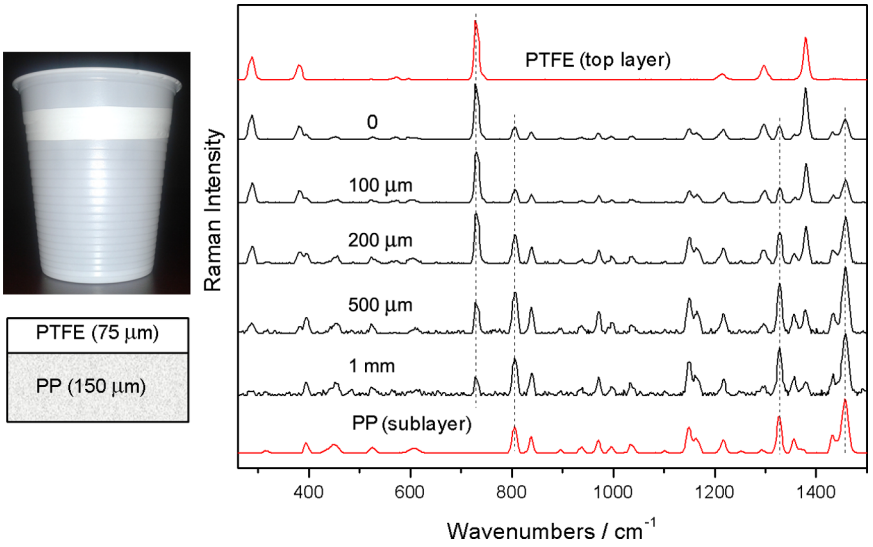

Figure 2. S1 sample: (left) image and stratigraphic scheme of the sample and (right) defocused Raman spectra shown for different distances from the "imaged" plane indicated next to each spectrum ($\Delta z = 0$, "imaged" position). The spectra are offset for clarity. Note the line markers are for guidance to emphasize the changing relative intensity of polytetrafluoroethylene (PTFE) and polypropylene (PP) with the defocusing distance; the reference spectra (the top and bottom, shown in red) are acquired on the sample cross section using conventional Raman spectroscopy.

here. Both the "imaged" and "defocused" spectra were acquired with acquisition times ranging from 10 to 20 s with 10 accumulations used (i.e., the total acquisition time per sample position was 100−200 s). Raw spectra of wheat seed and paper are presented with no background correction and no relative rescaling applied. The spectra of polymers are baseline corrected, but no relative rescaling is applied.

Conventional Raman Measurements. The Raman maps of cross sections were acquired with a Senterra dispersive micro-Raman spectrometer (Bruker) with a 1200 grooves/mm grating and a Peltier cooled CCD detector. The laser excitation wavelength was 785 nm with a power at the sample between 10 and 25 mW. The Raman maps were obtained with a 50× objective by collecting spectra with a step size between 1 and 3 μm along the x and y axes, exposure time of 5 s, and 10 accumulations, with a total time ranging from 1 to 8 h depending on the map size.

Optical Microscopy. Microscopic observations in reflected light were carried out using a Leitz Ortholux microscope with Ultropack illuminator equipped with a digital image capturing system.

Scanning Electron Microscopy (SEM) with Energy Dispersive X-ray Analysis (EDX). The electron microscopy and X-ray investigations were performed using a JEOL 5910LV microscope equipped with an X-ray spectrometer IXRF Systems/EDS 2000. The observations were carried out using backscattered electrons. The specimen chamber was maintained at low vacuum (28 Pa), and the accelerating voltage was 20 kV. The EDX maps and qualitative spectra have been registered from 0 to 20 kV and at $1-3 \times 10^{-7}$ A.

RESULTS AND DISCUSSION

The first conceptual demonstration of the extension of micro-SORS to resolve thin layers was performed on a two layer polymer system (S1) composed of PP drinking cup covered with a PTFE tape (Figure 2). Conventional Raman analysis performed on each layer separately confirmed the nature of the two polymeric compounds: polypropylene (PP) for the plastic cup sublayer, with the most intense sharp peaks at 806, 1327, and

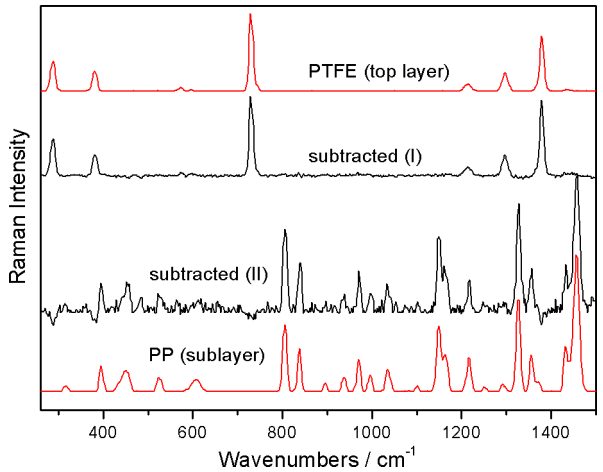

Figure 3. S1 sample: Numerical recovery of pure Raman spectra of individual layers from the micro-SORS measurements carried out on the two-layer polymeric system: (I) recovered top layer spectrum and (II) recovered sublayer spectrum. Reference spectra are shown in red (top and bottom).

1457 cm^{-1}, and PTFE with very sharp bands unequivocally distinguishable from the PP peaks (e.g., at 728 and 1379 cm^{-1}).

The micro-SORS spectrum in the "imaged" position ("0") was dominated by the contribution from the top layer, namely, PTFE, although low intensity peaks of the bottom layer, namely, PP, were also clearly visible. As the sample was displaced from its "imaged" position, the contribution of the sublayer (PP) gained in prominence over the top layer (PTFE).

The relative intensity change between the top and the bottom layer with defocusing is evidence for the presence of two separate layers rather than a single layer with superimposed contributions from two chemically different materials. The rate of evolution of individual signals also informs us on the order in which these layers are located within the sample; the top layer signal diminishing in relative strength over the sublayer signal with increasing defocusing distance Δz. The relative intensity change also enables us to separate the spectra into pure components

DOI: 10.1021/acs.analchem.5b01080
Anal. Chem. 2015, 87, 5810−5815

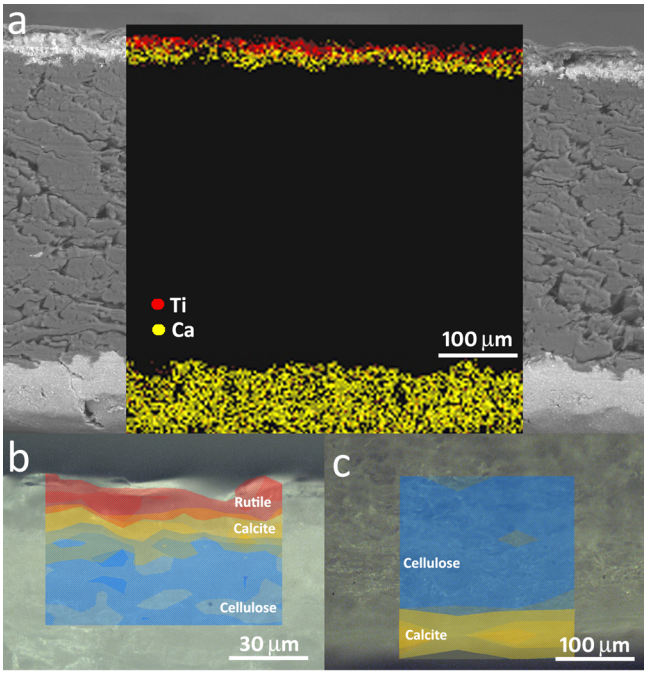

Figure 4. S2 sample: distribution of rutile (TiO_2), calcite ($CaCO_3$), and cellulose in a cross section. SEM image and elemental EDX map of the whole cross section (inset) (a) and Raman maps of the top (glossy side) (b) and bottom (back side) (c) of the cross section.

belonging to individual layers by scaled subtraction canceling the residual spectral contribution of the nontargeted layer as described earlier. This is illustrated in Figure 3 where the pure signatures of individual layers were recovered by this approach noninvasively. It should also be noted that all this is performed "blind" with no a priori knowledge of the composition of individual layers. Both the top layer and sublayer Raman signatures have been recovered successfully by this procedure exhibiting good accordance with pure reference Raman spectra of individual layers.

A second demonstration of the applicability of micro-SORS to resolve thin layers was carried out on a glossy paper sheet (S2). A test sample analyzed here consisted of a one-sided glossy paper. An inspection carried out with scanning electron microscopy (SEM) and with conventional Raman spectroscopy applied to a sample cross section (Figure 4) reveals the presence of a different composition in the glossy side compared to the back side. On the glossy side, two layers were detected: the external one, approximately 15 μm thick containing rutile (TiO_2), and the internal one, consisting of calcite ($CaCO_3$) also being 15 μm thick. There is a zone, a few micrometers thick between the two layers, where rutile and calcite are mixed. A 400 μm thick layer of pure cellulose is located below this stratigraphy. The back side shows only a single overlayer, approximately 80 μm thick, consisting of calcite.

Figure 5 reports the results on micro-SORS defocusing measurements performed both on the glossy (a) and on the back (b) sides. The micro-SORS spectrum in the "imaged" position ("0") acquired from the glossy side (a) shows the contribution from both the external and the internal layers, namely, rutile and calcite, respectively, identified through their Raman bands at 445 and 608 cm^{-1} (rutile) and 1086 cm^{-1} (calcite). In line with expectations, the contribution of the rutile (external layer) is dominant. As the sample is displaced from its "imaged" position and moved farther away from the microscope objective, the contribution of an internal layer (calcite) relative to the surface layer (rutile) increases. At displacements between 200 μm and 1 mm, very low intensity cellulose bands at 379 and 1118 cm^{-1} appear, revealing also the deepest portion of the paper.

The results of micro-SORS measurements performed on the back side (b) allow one to clearly discriminate the two present layers. The Raman spectrum in the "imaged" position is dominated by contribution from the top layer, calcite. Moving the sample farther away from the microscope objective accentuates the inner layer composed of cellulose.

In the final example, a wheat seed was analyzed (S3). The structure of the seed is shown in Figure 6a, where the external envelope and the more internal kernel are depicted. Both the microscopic observations and Raman mapping on a sample cross section reveal the presence of three layers (Figure 6b,c). The external layer, approximately 25 μm thick, is the pericarp and exhibits a high level of fluorescence, in accordance with observations of other studies. This prevented the detection of

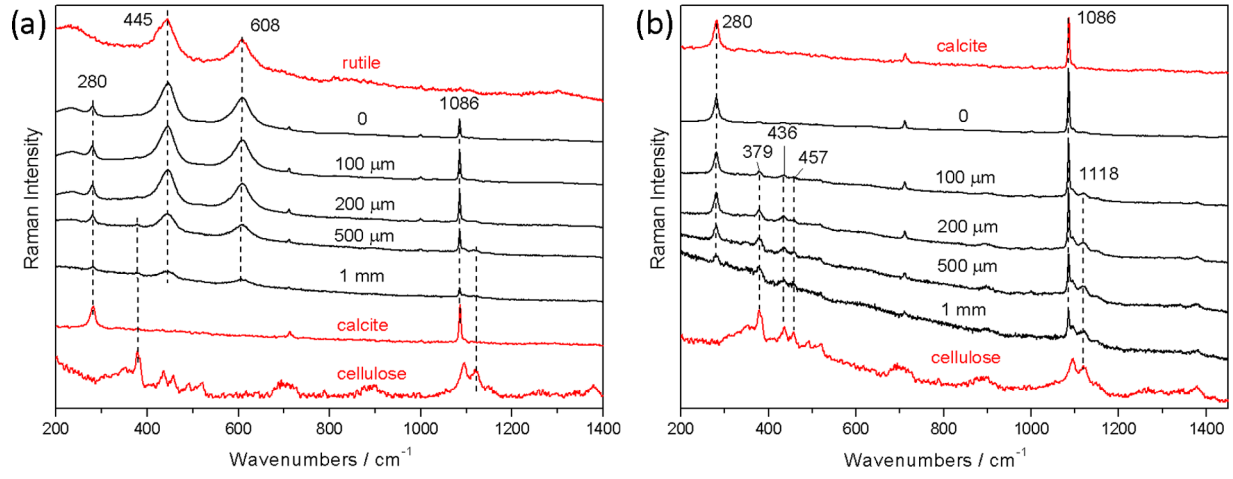

Figure 5. S2 sample: defocused Raman spectra of the glossy (a) and of the back (b) sides shown for different distances from the "imaged" plane indicated next to each spectrum ($\Delta z = 0$, "imaged" position). The spectra are offset for clarity. Note the line markers are for guidance to emphasize the changing relative intensity of rutile, calcite, and cellulose with the defocusing distance; the reference spectra are labeled "rutile", "calcite", and "cellulose" (shown in red) and were acquired on the sample cross section using conventional Raman spectroscopy.

DOI: 10.1021/acs.analchem.5b01080
Anal. Chem. 2015, 87, 5810−5815

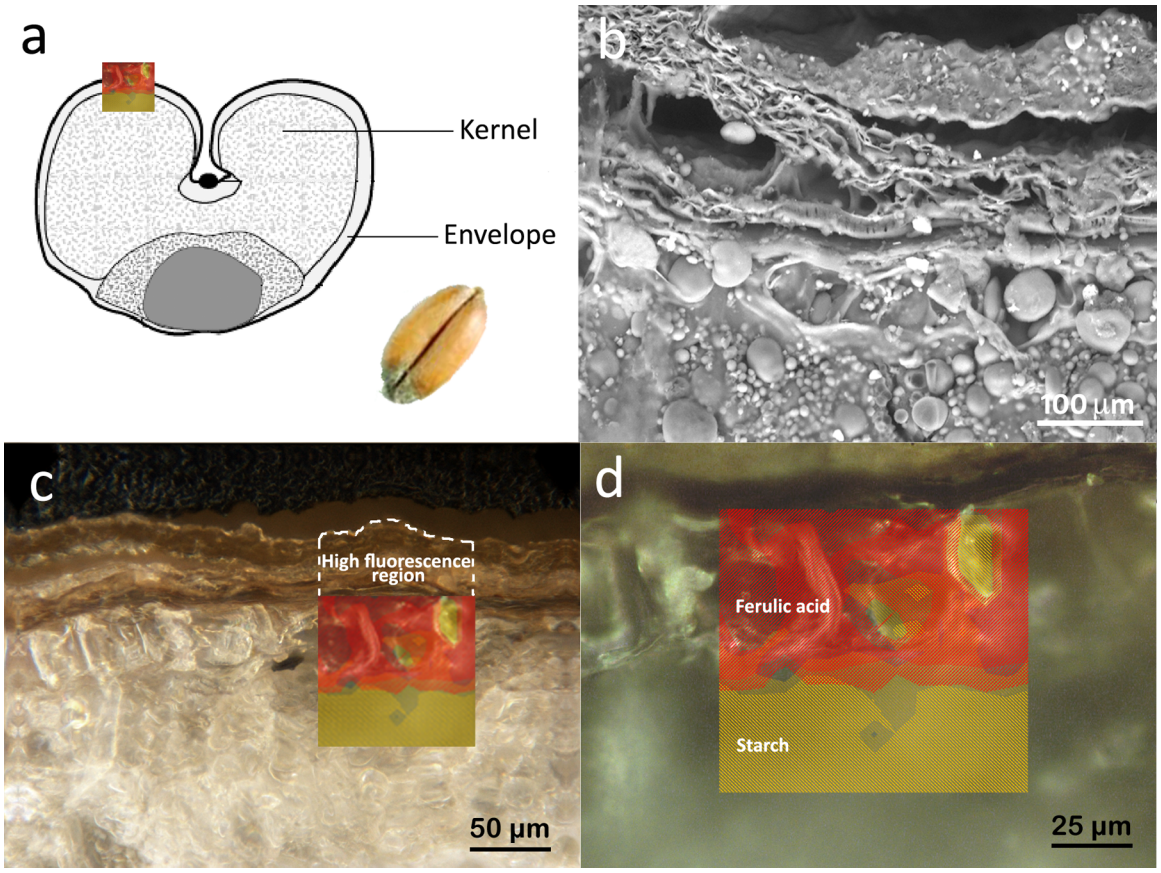

Figure 6. S3 sample: scheme of the wheat seed (the Raman map inset is used only to illustrate conceptually the approximate location on the grain surface where the mapping was performed) (a), SEM image of the cross section (b) and distribution of ferulic acid ($C_{10}H_{10}O_4$) and starch on the cross section visualized by the micro-Raman map (c and d).

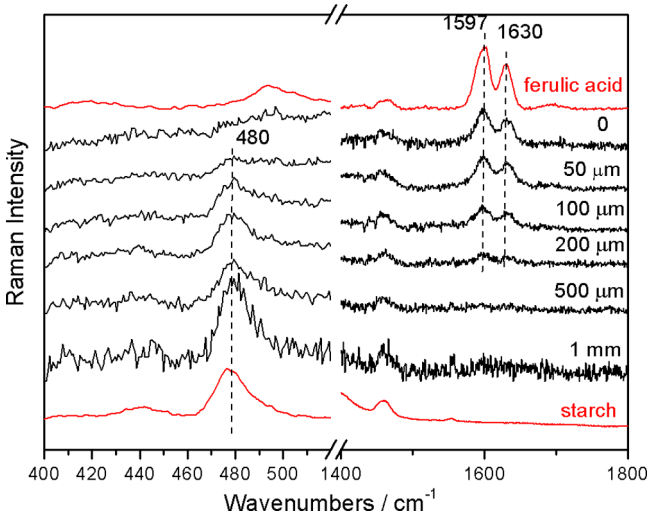

Figure 7. S3 sample: defocused Raman spectra shown for different distances from the "imaged" plane indicated next to each spectrum (Δz = 0, "imaged" position). The spectra are offset for clarity. Note the line markers are for guidance to emphasize the changing relative intensity of ferulic acid and starch with the defocusing distance; the reference spectra, shown in red, were acquired on the sample cross section using conventional Raman spectroscopy.

Raman signal from this layer alone in cross sectional analysis.[20] The thickness of the second layer, the aleurone layer, is approximately 50 μm and the spectrum of this layer is dominated by the Raman signature of ferulic acid ($C_{10}H_{10}O_4$). The last and more internal substance is the starch of the endosperm.

Micro-SORS measurements on this sample (Figure 7) have been carried out starting from the "imaged" position ("0"). In line with expectations, the Raman spectrum in the "imaged" position is dominated by contribution from the ferulic acid layer, with two sharp bands at 1597 and 1630 cm^{-1} originating from the aromatic ring and the C═C stretching modes near the surface of the grains, i.e., the aleurone cell layer. No Raman signal was detected from the highly fluorescing region of pericarp in line with expectations. (It should be noted that the "imaged" spectrum is a composite of signals from the surface thin fluorescent layer and the second layer dominated by the Raman signal of ferulic acid. The smaller depth resolution in this measurement than the lateral resolution in cross sectional analysis permits the observation of the ferulic acid layer despite top layer fluorescence.) When moving the sample surface away from the microscope objective, the contribution of starch strongly increases with the main broad band at 480 cm^{-1}, and the peaks of the ferulic acid dramatically decrease, up to a point where no Raman signal from ferulic acid is visible anymore. The 480 cm^{-1} band originates from the skeletal vibrations of the glucopyranose ring of starch, which is a major component of the endosperm layer of the grain. The measurements have been repeated at different points on the seed surface, and at each point, a very similar evolution was observed. All these observations were consistent with the above-mentioned cross sectional Raman analysis.

DOI: 10.1021/acs.analchem.5b01080
Anal. Chem. 2015, 87, 5810−5815

It should be noted that sample lateral heterogeneity can be a challenging issue if present at an excessive level as it could lead to misinterpretation of depth information. In such a situation, performing scans at several different locations on a sample surface can be used to inform one on the scale of present lateral heterogeneity and to mitigate against its adverse effects.[3] No such effects have been encountered with the samples analyzed in this study though. Overall, the examples given here illustrate the wide range of potential applications of micro-SORS.

CONCLUSIONS

Selected examples of micro-SORS have been demonstrated outside its field of inception, cultural heritage. These include the noninvasive analysis of stratified layers in polymer thin layers and films and analysis of layers in paper and biological specimens. These serve as examples to illustrate the very wide range of applications for micro-SORS. The method represents a new Raman imaging modality extending the accessible depths beyond those available with conventional Raman microscopy.

AUTHOR INFORMATION

Corresponding Authors

*Tel: +39 (0)2 66173326. E-mail:c.conti@icvbc.cnr.it.
*Tel: +44 (0)1235 445377. E-mail: pavel.matousek@stfc.ac.uk.

Notes

The authors declare no competing financial interest.

REFERENCES

(1) Dieing, T.; Hollricher, O; Toporski, J. *Confocal Raman Microscopy*; Springer: Berlin, 2011.
(2) Conti, C.; Colombo, C.; Realini, M.; Zerbi, G.; Matousek, P. *Appl. Spectrosc.* **2014**, *68*, 686.
(3) Conti, C.; Colombo, C.; Realini, M.; Matousek, P. *J. Raman Spectrosc.* **2015**, *46*, 476.
(4) Matousek, P.; Clark, I. P.; Draper, E. R. C.; Morris, M. D.; Goodship, A. E.; Everall, N.; Towrie, M.; Finney, W. F.; Parker, A. W. *Appl. Spectrosc.* **2005**, *59*, 393.
(5) Matousek, P.; Morris, M. D.; Everall, N.; Clark, I. P.; Towrie, M.; Draper, E.; Goodship, A.; Parker, A. W. *Appl. Spectrosc.* **2005**, *59*, 1485.
(6) Buckley, K.; Matousek, P. *Analyst* **2011**, *136*, 3039.
(7) Das, B. B.; Liu, F.; Alfano, R. R. *Rep. Prog. Phys.* **1997**, *60*, 22.
(8) Hebden, J. C.; Gibson, A.; Yusof, R.; Everdell, N.; Hillman, E. M. C.; Delpy, D. T.; Arridge, S. R.; Austin, T.; Meek, J. H.; Wyatt, J. S. *Phys. Med. Biol.* **2002**, *47*, 4155.
(9) Koizumi, H.; Yamashita, Y.; Maki, A.; Yamamoto, T.; Ito, Y.; Itagaki, H.; Kennan, R. *J. Biomed. Opt.* **1999**, *4*, 403.
(10) Owens, P. K.; Johansson, J. *Anal. Chem.* **2000**, *72*, 740.
(11) Pfefer, T. J.; Schomacker, K. T.; Ediger, M. N.; Nishioka, N. S. *Appl. Opt.* **2002**, *41*, 4712.
(12) Quan, L.; Ramanujam, N. *Opt. Lett.* **2002**, *27*, 104.
(13) Matousek, P.; Conti, C.; Colombo, C.; Realini, M. *Appl. Spectrosc.* **2015**, in press.
(14) Workman, J. J. *Appl. Spectrosc. Rev.* **2001**, *36*, 139.
(15) Wetzel, D. L.; Reffner, J. A. *Cereal Foods World* **1993**, *38*, 9.
(16) Jaaskelainen, A. S.; Holopainen-Mantila, U.; Tamminen, T.; Vuorinen, T. *J. Cereal Sci.* **2013**, *57*, 543.
(17) Eliasson, C.; Claybourn, M.; Matousek, P. *Appl. Spectrosc.* **2007**, *61*, 1123.
(18) Eliasson, C.; Macleod, N. A.; Jayes, L. C.; Clarke, F. C.; Hammond, S. V.; Smith, M. R.; Matousek, P. *J. Pharm. Biomed. Anal.* **2008**, *47*, 221.
(19) Hooijschuur, J.-H.; Iping Petterson, I. E.; Davies, G. R.; Gooijer, C.; Ariese, F. *J. Raman Spectrosc.* **2013**, *44*, 1540.
(20) Piot, O.; Autran, J. C.; Manfait, M. *J. Cereal Sci.* **2000**, *32*, 57.

DOI: 10.1021/acs.analchem.5b01080
Anal. Chem. 2015, 87, 5810−5815